P1.10 A Method to Illustrate and Measure the Relative Sensitivity of RCMs to Uncertainties in the Physics Parameterizations and the Large-Scale Forcing

Jian-Wen Bao[1*] S.A. Michelson[1, 2]

[1]NOAA/Earth System Research Laboratory, Boulder, Colorado

[2]CIRES, University of Colorado, Boulder, Colorado

1. INTRODUCTION

Simulations of regional high-resolution climate scenarios are becoming more and more important for local resource management and environmental impact assessment. All regional climate models (RCMs) are developed based on regional numerical weather prediction (NWP) models. Therefore, RCMs are sensitive to the uncertainties in the lateral boundary conditions and the physics parameterizations just as NWP models are. Since regional climate over land is the result of the interaction between the large-scale flow and the local scale forcing exerted by the topography and the inhomogeneity of the land surface, it is important to quantify the relative sensitivities of an RCM to the uncertainties in the specification of the large-scale flow and to those in the physics parameterization.

This paper presents a case study to illustrate a method for measuring the relative sensitivities of an NWP model to the uncertainties in the lateral boundary forcing and to those in the physics parameterizations, particularly in the land-surface parameterization. In this case study, simulations of the low-level winds in Central California are performed using the Weather Forecasting and Research (WRF) model, and the results of the simulations are compared with the wind profiler and surface observations during an IOP of the 2000 Central California Ozone Study (CCOS). These comparisons are intended to reveal the sensitivity of the simulated low-level winds in the Central Valley (CV) of California to the large-scale atmospheric forcing and soil initial conditions that are derived from the NCEP and ECMWF analyses. This case study is motivated by the fact that it has become very appealing to develop an RCM based on the WRF model because of the availability of high-order numerical schemes and extensive physics parameterization options in the WRF model.

* *Corresponding author address*: Jian-Wen Bao, NOAA/ERSL, 325 Broadway, Mail Stop: PSD3, Boulder 80305, CO; e-mail: Jian-en.Bao@noaa.gov.
the WRF model.

2. CASE STUDY

The analysis of both the observations and the simulations (Bao et al. 2007) has revealed several mesoscale low-level flow features in the CV (see Fig.1): (1) incoming low-level marine air flow through the Carquinez Straight into the Sacramento River delta, (2) diurnal cycle of upslope/downslope flows (3) up- and down-valley flow in the northern CV or hereafter referred to as the Sacramento Valley (SV), (4) the nocturnal low-level jet in the southern CV which is often referred to as the San Joaquin Valley (SJV), and (5) the Fresno and Shultz Eddies. All these flow features interact with each other on the scales of the entire CV and the local dominant slope of the topography. Conceptually, the intensity and variation of the incoming marine flow are controlled by the large scale pressure pattern and the thermal state of soil in the CV. The incoming marine flow interacts with the local anabatic/katabatic flows forced by topography, which are in turn subject to the modification of the local land-surface conditions and the impact of the valley-scale incoming marine flow. Therefore, it is important to reveal and understand the sensitivity of the simulated low-level winds to the uncertainties in the atmospheric and soil initial conditions.

The WRF simulations are carried out on three one-way nested domains at 36-, 12- and 4- km resolution. There are 50 vertical stretched levels with 30 levels within the lowest 2 km and the lowest model level at about 12 meters above the surface. The 4-km domain encompasses the CCOS field study area, which extends from the Pacific Ocean in the west to the Sierra Nevada in the east, and from north of Redding, CA, to south of the Mojave Desert. All three domains use the Eta PBL and surface layer schemes and the NOAH land surface model (LSM), along with the Dudhia short-wave, RRTM long-wave radiation parameterizations. The Lin et al. parameterization scheme is used on all three domains, and the Kain-Fritsch convective parameterization scheme is used on the 36-km and 12-km domains, no parameterization scheme is used on the 4-km domain.

Two simulations are carried out in which the initial and boundary conditions for the 36-km domain are generated using the 6-hourly 40-km AWIP analysis from the National Centers for Environmental Prediction (NCEP) and the 0.5-degree analysis from the European Centre for Medium-Range Weather Forecasts (ECMWF). The simulations are initialized at 12 UTC 29 July and run for 120 h, ending at 12 UTC 3 August 2000. Two more WRF simulations are conducted to investigate the sensitivity of the simulated low-level winds to the uncertainties in the atmosphere and soil initialization. In these two simulations, the initial and boundary conditions are created by permutating the atmospheric information and the soil information from the NCEP and ECMWF analyses (see Table 1). It is assumed here that the uncertainties in the soil initialization are more responsible for the errors in the simulated major driving force for the local anabatic/katabatic flows along the foothills in the CV than the uncertainties in the atmospheric initialization, while the uncertainties in the atmospheric initialization are more responsible for the errors in the simulated flow on the scale of the entire CV than the uncertainties in the soil initialization.

3. METHODOLOGY

Our method requires the use of scatter diagrams. In each scatter diagram, the abscissa is the prognostic variable from the AWIP simulation, and the ordinate is the counterpart from a perturbed simulation (i.e., either the AWIP AIR ECMWF SOIL or the ECMWF AIR AWIP SOIL simulation). Each data point in the scatter diagram corresponds to one of the 120 hours in the simulation. The interpretation of the scatter diagrams can be given in terms of simple linear regression (see Wilks 1995, section 6.2), in which the slope parameter indicates the linear response of the prognostic variable to the perturbation (either to the atmospheric initialization or to the soil initialization), the intercept parameter (*b*) measures the overall bias of the prognostic variable from the perturbed simulation relative to the AWIP simulation, and the coefficient of determination (R^2) provides a measure of the nonlinear response of the prognostic variable to the perturbation. The linear response to the perturbation is greater (less) when the slope parameter is farther (closer) from (to) unit. The nonlinear response is greater (smaller) when the coefficient of determination is smaller (greater).

In their statistical meaning, scatter diagrams provide a measure of the correlation between two simulations. We use this correlation to quantify the sensitivities of the simulations to the uncertainties in the analysis used to specify the atmospheric initial/boundary conditions and the initial soil conditions.

Table 1 Naming conventions for the WRF simulations. The first row and the first column indicate how each simulation is initialized (e.g., in the AWIP AIR ECMWF SOIL simulation, the 40 km NCEP AWIP analysis is used to initialize the atmosphere, while the soil is initialized using the 0.5-degree ECMWF analysis).

	AWIP ATMOSPHERE	***ECMWF ATMOSPHERE***
AWIP SOIL	AWIP	ECMWF AIR AWIP SOIL
ECMWF SOIL	AWIP AIR ECMWF SOIL	ECMWF

4. RESULTS

Overall, the sensitivity illustrated by scatter diagrams varies with different locations in the CV. Such variation demonstrates a noticeable trend from south to north in the CV, depending on where the location is relative to the San Francisco Bay Area and the foothills. In this presentation, only the scatter diagrams at three representative locations in the CV are shown and discussed.

Figure 2 contains the scatter diagrams for the u- and v-components of the winds averaged from the surface to 300 m above ground level (AGL) at Bakersfield, which is located in the southern SJV (labeled as BKF in Fig. 3). It is seen that the slope parameters associated with the u-component of the wind for the perturbation to the soil conditions (in blue) are closer to unit (0.8077) than those for the perturbation to the atmospheric conditions (in red, 0.7176), indicating the sensitivity to the soil conditions is smaller than the sensitivity to the atmospheric conditions. For the v-component of the wind, the slope parameters are comparable (0.5708 for the perturbation to the soil conditions and 0.5879 for the perturbation to the atmospheric conditions), indicating that the sensitivity to the soil conditions and the sensitivity to the atmospheric conditions are similar. Thus, the low-level v-component of the wind is more influenced by the combined effect of the soil thermal dynamics and the valley-scale flow than the u-component of the wind, which is more influenced by the orographic blocking of the valley-scale flow. The nonlinear response of the winds averaged from the surface to 300 m AGL at this particular location, as measured by the size of the coefficient of determination, is stronger for the perturbation to the atmospheric conditions than the soil conditions. The biases (i.e., the intercept parameters) relative the AWIP run are small enough to be ignored. Further spectral analysis of the variances of the u- and v-components indicates that the nonlinear response is mostly associated with the power of the variances on the temporal scales shorter than 24 hours (not shown), whose predictability in a complex orographic environment like the CV is shown to be very poor (see, e.g., Rife et al. 2004).

The scatter diagrams for the winds averaged between the surface and 300 m AGL at Redding, which is located in the SV (labeled as RDG in Fig. 3), are presented in Fig. 4. For both the u- and v-components of the wind, the slope parameters are closer to unit for the perturbation to soil conditions than the perturbation to the atmospheric conditions (0.8641 versus 0.3492 for the u-component and 0.9117 versus 0.8158 for the v-component) indicating that at Redding, the low-level winds are more sensitive to the atmospheric conditions. However, the difference between the slope parameters for the perturbation to the atmospheric conditions and perturbation to the soil conditions for the u-components is smaller and the slope parameters are closer to unit than for the v-component, indicating that the v-component of the winds is not as sensitive to both the soil and atmospheric conditions as the u-component. This can be explained by the fact that the dominant flow at Redding in this case is caused by the diurnal change of the up-valley, down-valley flow, which is dynamically influenced by the topography to the north. Since this flow is predominately in the v-direction (along the valley), it is sensible that the v-component would not be as sensitive to either the atmospheric or the soil conditions in the CV as the u-component. It is also interesting to note that the slope parameters for both the u- and v- components of the 300-m AGL averaged winds are closer to unit for the perturbation to the soil conditions in Redding than they are at Bakersfield, indicating that at Redding the 300-m AGL averaged winds have less influence from the soil thermal dynamics than at Bakersfield. This may be explained by the fact that Redding is closer to the San Francisco Bay Area than Bakersfield. Thus, the valley-scale flow, which is mainly forced by the incoming marine flow through the San Francisco Bay Area, has more of a direct impact on the low-level winds at Redding than at Bakersfield. Conversely, since Bakersfield is farther from the San Francisco Bay Area, the incoming flow is more likely to be modified by the local land/surface processes than at Redding. The nonlinear response at Redding for both the u- and v- components of the 300 m AGL averaged winds are, as at Bakersfield, greater to the perturbation to the atmospheric conditions. However, the non-linear response to the perturbation to the soil conditions is less at Redding than at Bakersfield**,** therefore there is more of a non-linear response to the soil initialization at Bakersfield that at Redding.

Figure 5 presents the scatter diagrams of the winds averaged between the surface and 300 m AGL at Sacramento (labeled as SAC in Fig. 3). The overall sensitivity at this location is different from that at either Bakersfield or Redding. For the winds averaged over the lowest 300 m AGL, the slope parameter of the u-component of the wind is farther from unit for the perturbation to the soil conditions than for the atmospheric conditions (0.6301 for the perturbation to the soil conditions and 0.7429 for the perturbation to the atmospheric conditions), while the slope parameter of the v-component is closer to unit for the perturbation to the soil conditions (0.8987) than for the atmospheric conditions (0.3154). Given that Sacramento is just east to the San Francisco Bay Area, the u-component at this location is representative of the intensity of the incoming marine flow through the San Francisco Bay Area, while the v-component is representative of the north-south branching of the incoming flow. This characteristic of sensitivity reveals that the intensity of incoming marine flow is more influenced by the perturbation to the soil state within the CV, while the north-south branching of the incoming flow is more influenced by the atmospheric conditions. The non-linear response of both the u- and v- components of the 300-m AGL averaged winds at Sacramento is greater to the perturbation to the atmospheric conditions than to the perturbation to the soil conditions.

A naturally-raised question is whether in this case the variance caused by changing the analysis used for the specification of the atmospheric initial/boundary conditions and the initial soil conditions can be used to explain the variance of the errors in the WRF simulations. Figure 6 depicts the scatter diagrams for the simulated and observed winds averaged between the surface and 300 m AGL at Sacramento. On one hand, the similarity between Fig. 6 and Fig. 5 indicates that a significant part of the variance of the model errors shown in Fig. 6 can be explained by the variance of the uncertainties in the analysis used for specifying the large-scale forcing (via atmospheric initial/boundary condition) and the land-surface conditions (via the soil-state initialization). On the other hand, the quantitative difference between these two figures indicates that the variance shown in Fig.6 is greater than that in Fig. 5, strongly suggesting that the uncertainties in both the NCEP and ECWMF analyses and/or other model uncertainties may still be significant enough to affect the accuracy of the model simulations. Nevertheless, this result clearly illustrates the usefulness of the proposed measure for the uncertainties in diagnosing the errors sources of the model.

5. CONCLUSIONS

This paper demonstrates, by a case study, how scatter diagrams are used to measure the sensitivities of NWP models for regional climate simulations to the uncertainties/perturbations in the large-scale forcing and the physics parameterizations. In this approach, the abscissa of scatter diagrams is the prognostic variable from one simulation, and the ordinate is the counterpart from a perturbed simulation. Each data point in the scatter diagram corresponds to one output time in the simulation. The interpretation of the scatter diagrams can be given in terms of simple linear regression, in which the slope parameter indicates the linear response of the prognostic variable to the perturbation (either to the atmospheric initialization or to the soil initialization), the intercept parameter (b) measures the overall bias of the prognostic variable from the perturbed simulation relative to the unperturbed simulation, and the coefficient of determination (R^2) provides a measure of the nonlinear response of the prognostic variable to the perturbation. The linear response to the perturbation is greater (less) when the slope parameter is farther (closer) from (to) unit. The nonlinear response is greater (smaller) when the coefficient of determination is smaller (greater).

The results from this case study indicate that the low-level winds simulated by the WRF model, a typical NWP model, in the Sacramento Valley are more sensitive to the initialization of the atmosphere than that of the soil. Although the simulated low-level winds in the southern most part of the San Joaquin Valley are more sensitive to the soil initialization than the Sacramento, overall they are more sensitive to the atmosphere initialization than to the soil. This distribution of sensitivity indicates the important role that the incoming marine flow through the San Francisco Bay Area plays in controlling the local transport and dispersion of pollutants in the entire Central Valley. It is also shown that the incoming marine flow is more equally sensitive to the atmosphere and soil initialization than the winds in either the Sacramento Valley or the San Joaquin Valley.

It is a widely accepted notion that an accurate soil initialization is important to the simulation of locally forced low-level winds. Our study not only reinforces this notion but also strongly suggests that it is the interaction of the valley scale wind associated with the incoming marine air and the locally forced winds along the foothills that determines winds in the Central Valley and therefore the overall transport and dispersion of pollutants across the valley. Thus, future effort to improve the accuracy of the WRF simulated low-level winds in the Central Valley should focus on the identification of not only the error sources of the simulated locally forced winds but also the error sources of the along valley winds associated with the incoming marine flow through the San Francisco Bay Area.

6. REFERENCES

Bao, J.-W., S. A. Michelson, P. O. G. Persson, I. Djalalova, and J. M. Wilczak, 2006: Observed and simulated low-level winds in an episode case of the Central California Ozone Study. To be submitted to *J. of Appl. Meteor*.

Rife, D. L., C. A. Davis, Y. Liu, and T. T. Warner, 2004: Predictability of low-level winds by mesoscale meteorological models. *Mon. Wea. Rev.*, 132, 2553-2569.

Skamarock, W. C., J. B. Klemp, J. Dudhia, D. O. Gill, D. M. Barker, W. Wang, and J. G. Powers, 2005: A description of the Advanced Research WRF Version 2. NCAR Tech Notes-468+STR.

Wilks, D. S., 1995: *Statistical Methods in the Atmospheric Sciences*. Academic Press, 467 pp.

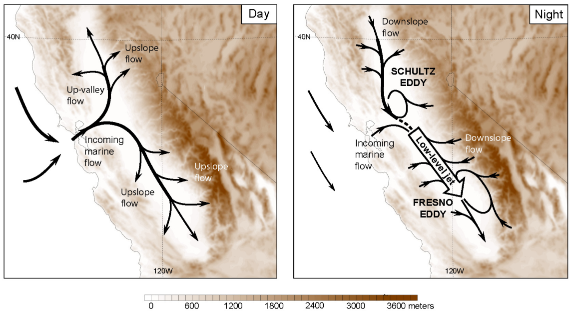

Figure 1: Conceptualization of the daytime and nighttime low-level wind regimes during the 5-day episode.

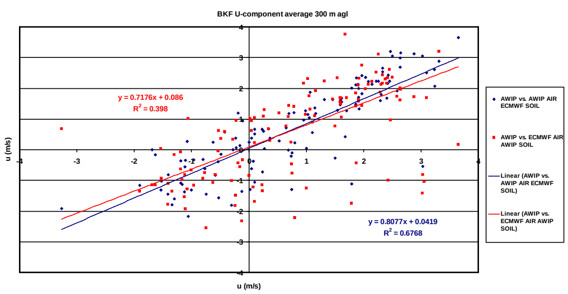

(a)

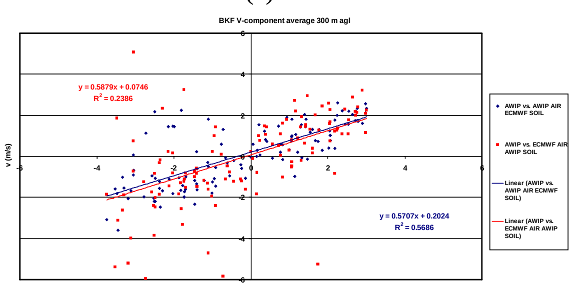

(b)

Figure 2: Scatter diagrams of the AWIP run vs. AWIP ECMWF AIR AWIP SOIL run (in red) and AWIP run vs. AWIP AIR ECMWF SOIL run (in blue), with linear regression information (i.e., the slope and the intercept parameters, and the coefficient of determination) for the winds averaged between the surface and 300 m AGL at Bakersfield, CA (BKF). Panel (a) is for the u-component and panel (b) is for the v-component.

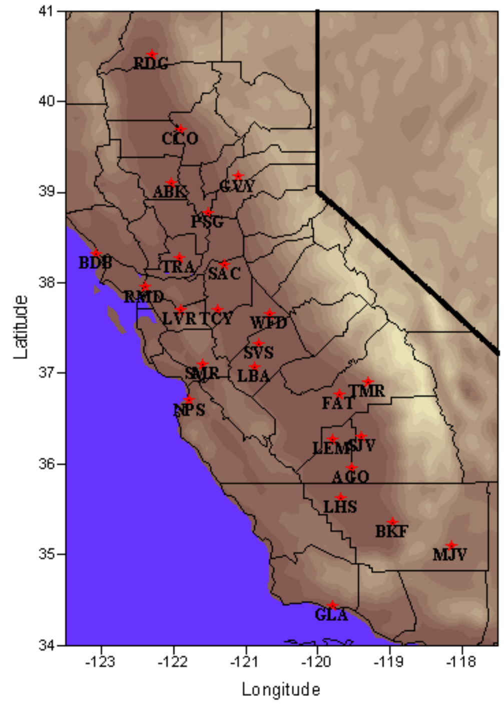

Figure 3: Map of California with the location of the 25 profiler sites in the CCOS field study.

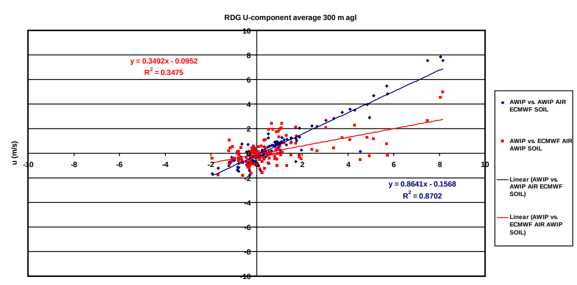

(a)

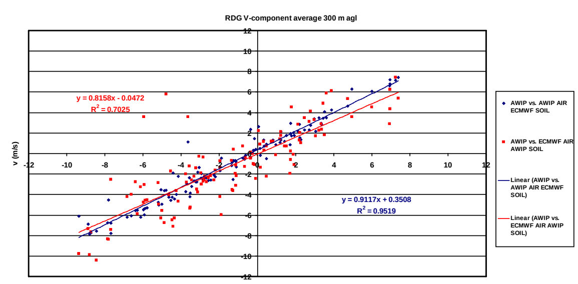

(b)

Figure 4: Same as Figure 2 except at Redding, CA (RDG).

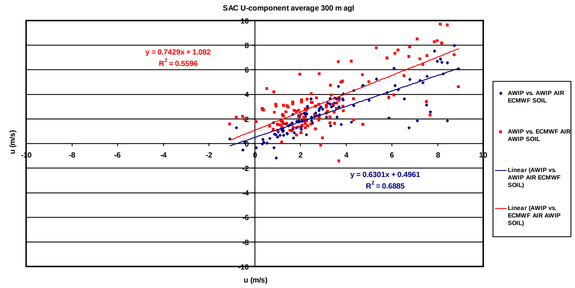

(a)

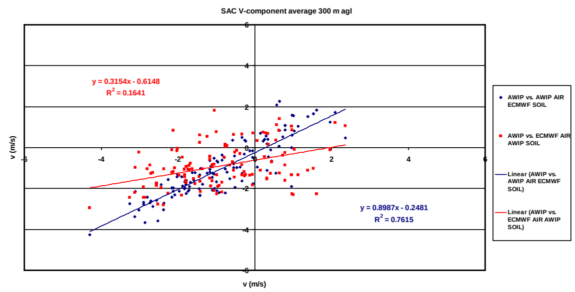

(b)

Figure 5: Same as Figure 2 except at Sacramento, CA (SAC).

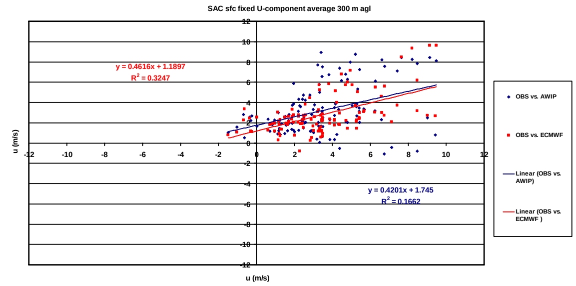

(a)

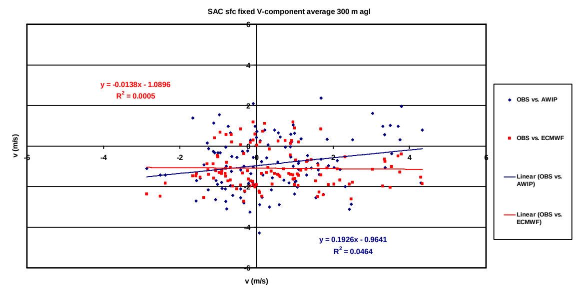

(b)

Figure 6: Scatter diagrams of both the AWIP run (in red) and the ECMWF run (in blue) vs observations, with linear regression information (i.e., the slope and the intercept parameters, and the coefficient of determination) for the winds averaged between the surface and 300 m AGL at Bakersfield, CA (BKF). Panel (a) is for the u-component and panel (b) is for the v-component.